# EXPLORING COMPRESSED BARYONIC MATTER — NUCLEUS–NUCLEUS COLLISIONS AT THE FUTURE FACILITY IN DARMSTADT*

Peter Senger

Gesellschaft für Schwerionenforschung (GSI)
Postfach 110552, 64220 Darmstadt, Germany

*(Received February 4, 2004)*

The study of high-energy nucleus–nucleus collisions will be one of the major activities at the future accelerator facility in Darmstadt. The goal of the research program is the exploration of the QCD phase diagram in the region of high baryon densities. Relevant experimental observables and the proposed detector system will be discussed.

PACS numbers: 25.75.Dw

## 1. The future accelerator facility in Darmstadt

The proposal for an International Accelerator Facility for Beams of Ions and Antiprotons in Darmstadt has been approved by the German Federal Government in February 2003. The facility will provide unique research opportunities in the fields of nuclear, hadron and plasma physics [1]. The accelerators will deliver primary beams (protons up to 90 GeV, Uranium up to 35 $A$GeV, nuclei with $Z/A = 0.5$ up to 45 $A$GeV) and secondary beams (rare isotopes and antiprotons) with high intensity and quality. The facility comprises a double-ring synchrotron, rings for accumulation, cooling and storage of primary and secondary beams, and dedicated detector arrangements. The research program includes the study of nuclei far from stability, hadron spectroscopy, the study of compressed nuclear matter, the investigation of plasmas induced by ion and laser beams and atomic physics. The layout of the facility is displayed in figure 1.

A major field of research will be the study of super-dense baryonic matter as produced in heavy-ion collisions at energies up to 45 $A$GeV. The aim of the experiments is to explore the QCD phase diagram at high net baryon

* Presented at the XXVIII Mazurian Lakes School of Physics, Krzyże, Poland, August 31–September 7, 2003.

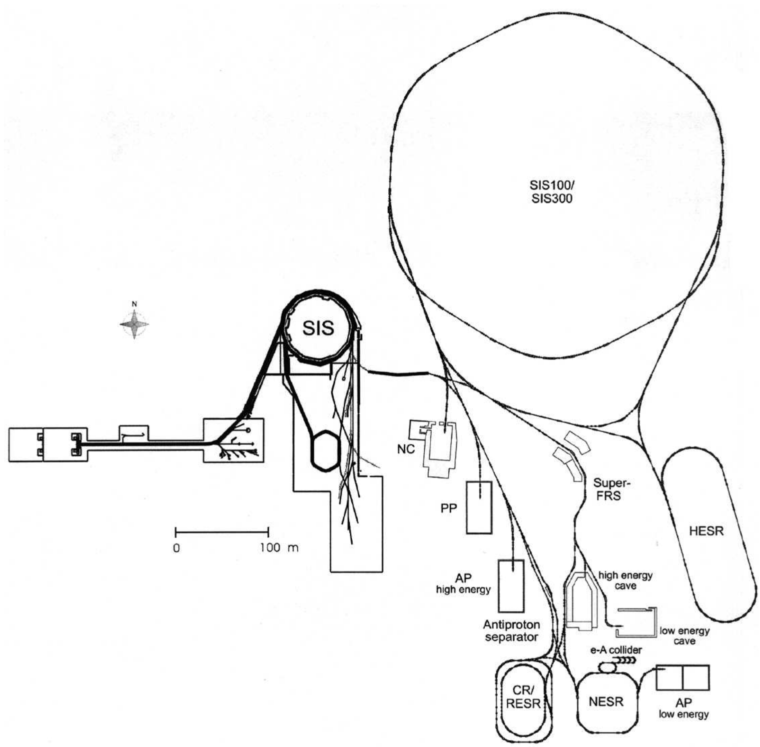


Fig. 1. Schematic layout of the existing (left part) and the planned accelerator facility at GSI (right part).

densities and moderate temperatures. This approach is complementary to the studies of matter at high temperatures and low net baryon densities performed at RHIC and LHC. The fundamental questions to be addressed by the proposed Compressed Baryonic Matter (CBM) experiment include:

— the search for in-medium modifications of hadrons which might indicate the onset of chiral symmetry restoration,

— the search for indications of the deconfinement phase transition from hadronic to quark–gluon matter at high baryon densities,

— the study the equation-of-state of baryonic matter at high densities.

These topics are of fundamental interest both for astrophysics [2] and the Quantum Chromo Dynamics (QCD) at high baryon densities [3].

## 2. Exploring the QCD phase diagram with heavy-ion collisions

In principle, new states of strongly interacting matter can be generated by compressing or heating nuclear matter. In the first case dense and cold baryonic matter is created with a large baryochemical potential like it exists in the core of a conventional neutron star. In the second case pions are produced, and nuclear matter is converted into (hot) hadronic matter with a small baryochemical potential. Similar conditions prevailed in the early universe. At very high densities or temperatures the baryons and mesons are expected to dissolve into quarks and gluons. The partonic matter has different baryochemical potentials depending on the creation process.

In the laboratory, hot and compressed baryonic/hadronic matter can only be created in collisions between heavy nuclei. This offers the possibility to vary density and temperature within certain limits. Figure 2 shows the maximum baryon density produced in central Au+Au collisions as function of time for different beam energies as calculated with a transport code [4]. Whereas the baryon density increases with increasing beam energy, the lifetime of the dense fireball decreases. If the high-density phase exists only for 2-3 fm/$c$ it might be very hard to observe it. Therefore, beam energies below 50 $A$GeV are best suited for the investigation of dense baryonic matter.

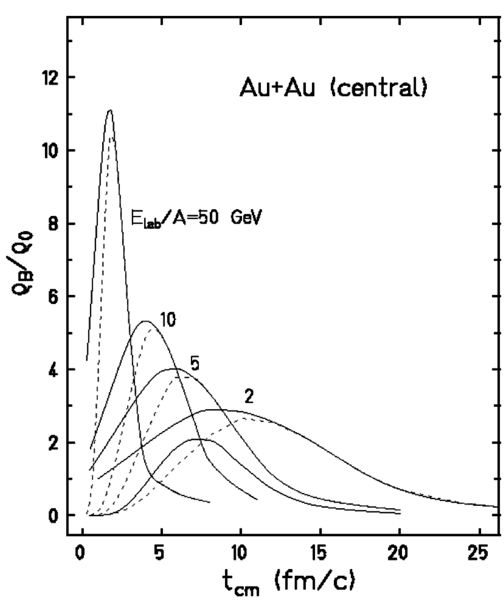


Fig. 2. Baryon density in units of saturation density in the center-of-mass system calculated for central Au+Au collisions as function of time for different beam energies. The dashed lines represent the densities of nucleons which suffered at least one collision (taken from [4]).

Moreover, the temperature increases also with beam energy. The temperature is reflected in the number of pions produced in the heavy ion collision. Figure 3 shows the pion multiplicity per participating nucleon measured in nucleus–nucleus (symbols) and nucleon–nucleon collisions (solid line) as function of the available energy in the c.m. system. At low beam energies, the pion-to-participant ratio is smaller in nucleus–nucleus collisions than in nucleon–nucleon collisions. This might be due to pion reabsorption which is favored at high baryon densities. At AGS energies (*e.g.* Au+Au collisions around 10 *A*GeV) the pion to baryon ratio is about 1 while it is about 5 in Pb+Pb collisions at the CERN-SPS energy of 158 *A*GeV. Again, the experimental observables from heavy ion collisions up to about 40 *A*GeV are expected to be more affected by the baryon density than at higher beam energies where the pions play an increasingly dominating role.

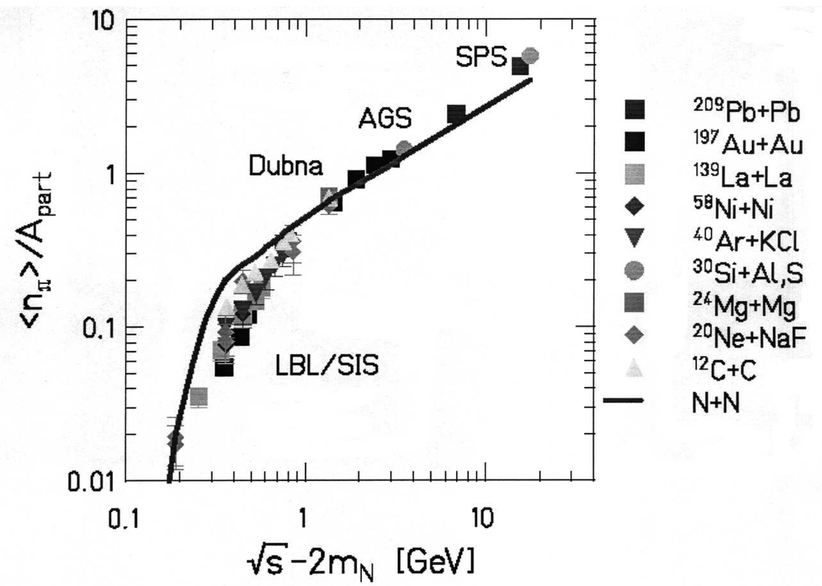


Fig. 3. Pion multiplicity per participating nucleon for nucleus–nucleus (symbols) and nucleon–nucleon collisions (solid line) as function of available energy in nucleon–nucleon collisions (taken from [5]).

The CERN-NA49 collaboration recently reported intriguing results from measurements performed at beam energies between 30 and 80 *A*GeV [6]. Figure 4 (left part) shows the $K^+/\pi^+$ ratio as function of the beam energy for Au+Au (Pb+Pb) collisions (solid points) and proton–proton collisions (open points). The kink in the heavy-ion data around 30 *A*GeV beam energy cannot be explained by transport models (RQMD, URQMD) and statistical hadron gas models (see Fig. 4 left part). Therefore, the authors speculate that the kink is caused by a deconfinement phase transition [7]. This interpretation is also in line with the observation that the slope of the $K^+$ meson spectra exhibits a constant value within the SPS energy range (see right part of figure 4). Again, transport models cannot explain the data and predict much lower values for the $K^+$ inverse slope parameters [8].

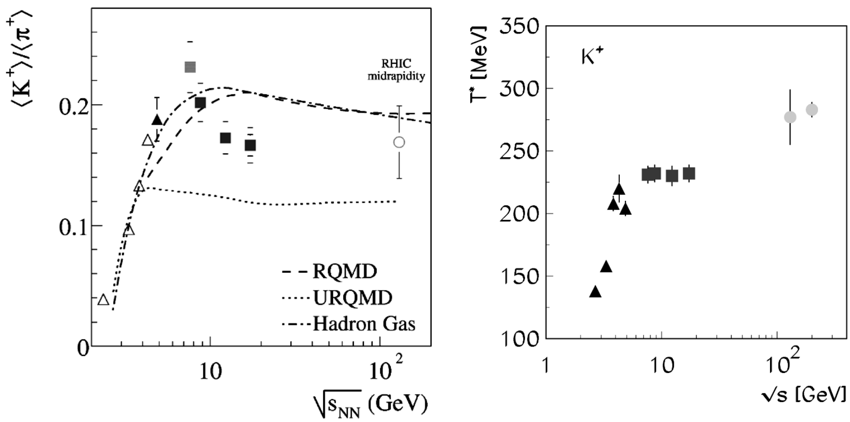


Fig. 4. Ratio of $K^+$ to $\pi^+$ meson total yields (left part) and inverse slope parameters of the $K^+$ spectra (right part) as function of beam energy measured in Au+Au and Pb+Pb collisions (full symbols) in comparison to data from proton–proton collisions (open symbols) (see [6]).

In order to study the phase diagram of strongly interacting matter one has to define thermodynamic variables such as temperature and the baryon chemical potential. These parameters are usually extracted from measured particle multiplicity ratios using the statistical model [9–11]. The resulting points derived from data taken at different beam energies are shown in figure 5 (full symbols). Note that these points correspond to the conditions at chemical freeze-out, *i.e.* when the particles cease to interact inelastically.

The statistical analysis of data measured in Pb+Pb and Au+Au collisions at the CERN-SPS and at RHIC indicates that a temperature of about 170 MeV is reached at chemical freeze-out. Above this temperature the hadrons are expected to dissolve forming a quark–gluon plasma. Future experiments at the Large Hadron Collider (LHC) at CERN aim at studying the properties of the quark–gluon plasma at even higher temperatures. In all these experiments the phases of hadronic matter are studied at extremely high temperatures and low net baryon densities, where the number of particles and anti-particles are approximately equal. This region of the phase diagram, which corresponds to the conditions in the early universe, is characterized by small values of the baryon chemical potential (see figure 5).

The solid curve along the freeze-out points in figure 5 represents a calculation with a constant baryon density (baryons + antibaryons) of about $\rho_B = 0.75\,\rho_0$ [12]. The curve labeled "Lattice QCD" represents the phase boundary between the quark–gluon plasma and the hadronic phase as obtained with a QCD lattice calculation [13] with a "critical point" at $T_c = 160 \pm 3.5$ MeV and $\mu_c = 725 \pm 35$ MeV. This calculation predicts a first order phase transition for values of $\mu_B$ larger than $\mu_c$ (solid line) and a smooth cross over for $\mu_B$ smaller than $\mu_c$ (dotted line). The discovery of the critical point would be a major step towards the understanding of the QCD phase diagram.

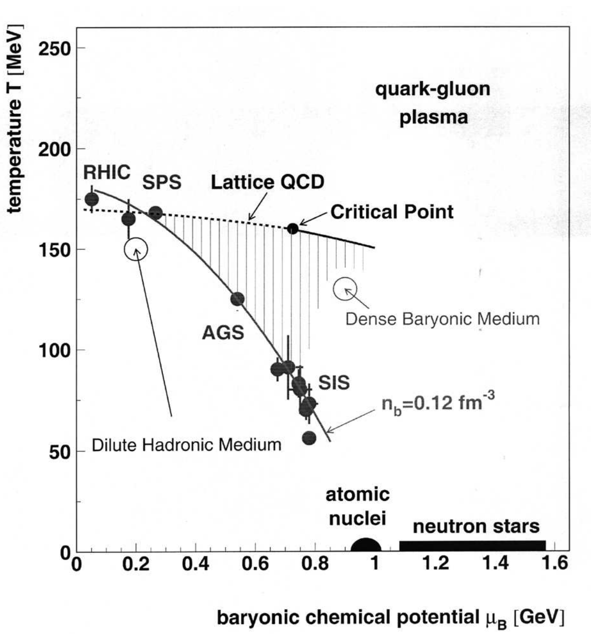


Fig. 5. The phase diagram of strongly interacting matter plotted as a function of temperature and baryochemical potential. Full symbols: freeze-out points obtained with a statistical model analysis from particle ratios measured in heavy collisions [9–11]. Curve labeled "Lattice QCD": phase transition predicted by a QCD lattice calculation [13]. "Dilute hadronic medium": $\rho_B = 0.038$ fm$^{-3} \approx 0.24\rho_0$. "Dense baryonic medium": $\rho_B$=1.0 fm$^{-3} \approx 6.2\,\rho_0$.

Figure 5 suggests that for CERN–SPS beam energies and above the transition from the quark–gluon plasma to hadronic matter and the chemical freeze-out occur almost simultaneously. Hence, large baryon densities are only accessible at beam energies significantly below SPS energies. This region of the QCD phase diagram — marked by the hatched area in figure 5 — is only little explored, both experimentally and theoretically. The future experimental challenge is to explore the region of high baryon densities beyond chemical freeze-out. This requires the measurement of penetrating probes such as electron–positron pairs which are emitted also prior to freeze-out and escape essentially undistorted from the compressed nuclear collision zone.

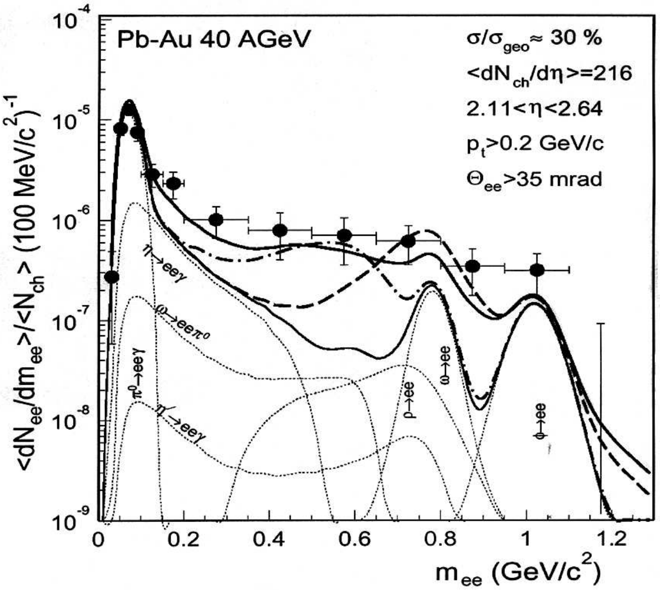


Fig. 6. Inclusive $e^+e^-$ pair mass spectrum, compared to the hadron decay cocktail (thin solid; individual contributions thin dotted) and to theoretical model calculations based on $e^+e^-$ annihilation with an unmodified $\rho$ (thick dashed), an in-medium dropping $\rho$ mass (thick dashed-dotted) and an in-medium spread $\rho$ width (thick solid). The model calculations contain the cocktail, but without the $\rho$ to avoid double counting. Taken from [14].

Up to now dilepton pair measurements have been performed in heavy-ion collisions at beam energies below 2 *A*GeV (DLS Berkeley ) and above 40 *A*GeV (CERN–CERES). The most recent result of the CERES collaboration is presented in figure 6 [14]. It shows the inclusive $e^+e^-$ pair mass spectrum measured in Pb+Au collisions at 40 *A*GeV together with the hadronic cocktail of known dilepton sources and with results of model calculations based on different assumptions on the in-medium properties of the $\rho$-meson. The error bars of the data — which contain less than 200 true dilepton pairs — are too large to rule out a particular theory on the in-medium properties of the $\rho$ meson. In order to draw final conclusions on the in-medium modifications of $\rho$ mesons a data set of approximately $10^5$ true dilepton pairs would be required. Such an amount of data can only be obtained at a dedicated facility.

## 3. The future nucleus–nucleus collision research program

The proposed heavy-ion collision experiment at the future facility will simultaneously measure observables which are sensitive to effects of high baryon densities and to phase transitions. In particular, we focus on the investigation of:

- Short-lived vector mesons. Their spectral properties, the mass and the width, can be studied in the dense nuclear medium by their decay into lepton pairs. Since the leptons are very little affected by the passage through the high-density matter, they provide, as a penetrating probe, almost undistorted information on the conditions in the interior of the collision zone [15]. These studies will substantially benefit from the experience presently gained in experiments with the electron spectrometer HADES at GSI.

- Charmonium production at beam energies close to the kinematical threshold. The $J/\psi$ mesons will be measured via their decay into electron–positron pairs. The multiplicity of $J/\psi$ mesons per participating nucleon as function of system size and beam energy is expected to be sensitive to the deconfinement phase transition.

- Open charm, *e.g.* $D$-mesons. The effective masses of $D$-mesons — a bound state of a heavy charm quark and a light quark — are expected to be modified in dense matter similarly to those of kaons. Such a change would be reflected in the relative abundance of charmonium ($c\bar{c}$) and $D$-mesons [16].

- Strange particles, in particular baryons (anti-baryons) which contain more than one strange (anti-strange) quark. Hyperons serve as a probe for high baryon densities.

- Macro-dynamical effects, like collective flow of nuclear matter during the expansion of the initially compressed system. Such probes provide constraints on the underlying equation of state which is of great significance *e.g.* for astrophysical problems. Moreover, the measurement of the flow of charmonium and multistrange hyperons will provide new information on the behavior of these rare probes in dense baryonic matter.

- Characteristic event-by-event fluctuations near the critical point. The identification of a critical point would provide direct evidence for the existence and the character of a deconfinement phase transition in strongly interacting matter.

- Search for exotic objects like pentaquarks, short-lived multi-strange objects [17], strongly bound kaonic systems [18], and precursor effects of a color super-conducting phase at very high baryon densities [19].

The challenge of the open charm measurements at the future facility is illustrated in Figure 7 which shows the production cross section of $D$- (and anti-$D$)-mesons in elementary collisions [20, 21]. The beam energies available at the new machine in Darmstadt range up to 90 GeV ($\sqrt{s} = 13.5$ GeV) for proton–proton collisions and up to 45 $A$GeV ($\sqrt{s} = 9.7$ GeV) for nucleus–nucleus collisions.

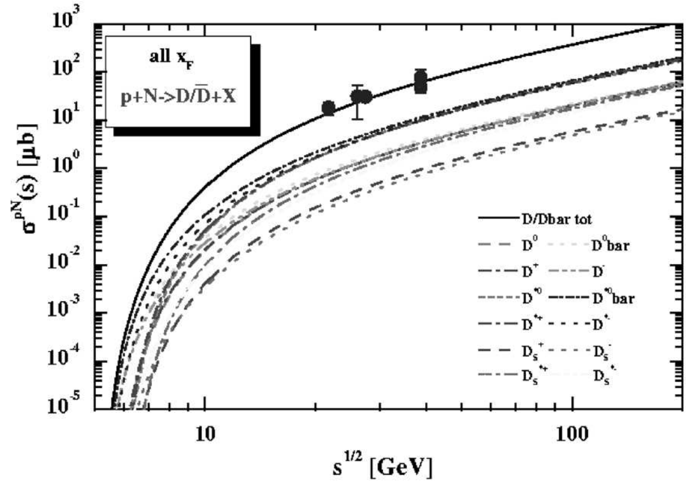


Fig. 7. Production cross sections of $D$- and anti-$D$-mesons in elementary reactions (taken from [21]).

The proposed experimental program includes:

- Compressed baryonic matter studies using nucleus–nucleus ($A + A$) collisions at beam energies ranging from 2–45 $A$GeV ($Z/A = 0.5$) and up to 35 $A$GeV for $Z/A = 0.4$.

- Reference measurements on the production of charm, strangeness and low-mass vector mesons in proton–nucleus collisions up to energies of 90 GeV.

- Measurement of elementary production cross sections of charm (charmonium, $D$-Mesons), light vector mesons, multistrange hyperons, and exotica like pentaquarks in proton–proton collisions at beam energies up to 90 GeV.

## 4. The CBM detector

The experimental task is to identify both hadrons and leptons and to detect rare probes in a heavy ion environment. The apparatus has to measure multiplicities and phase-space distributions of hyperons, light vector mesons, charmonium and open charm (including the identification of protons, pions and kaons) with a large acceptance. The challenge is to filter out those rare probes in Au+Au (or U+U) collisions at reaction rates of up to $10^7$ events per second. The charged particle multiplicity is about 1000 per central event. Therefore, the experiment has to fulfill the following requirements: fast and radiation hard detectors, large acceptance, electron and hadron identification, high-resolution secondary vertex determination and a high speed trigger and data acquisition system. The CBM detector will be a universal setup with unique properties.

The CBM experimental setup consists of the following detector components:

- Dipole magnet for bending the particle trajectories and d-ray deflection.
- Radiation hard Silicon pixel/strip detectors for tracking and vertex determination.
- Transition radiation detectors (TRD) for electron identification.
- Ring imaging Cherenkov detectors (RICH) for electron (and hadron) identification.
- Resistive plate counters (RPC) for time of flight measurement.
- Electromagnetic calorimeter for identification of electrons, photons and muons.
- Diamond pixel detectors for TOF start signal.

The Silicon tracking detectors (up to 7 layers) are placed inside a magnetic field. This technology is now sufficiently advanced, in particular because of the experimental efforts of the various LHC experiments, so that low mass and high mass lepton pairs can be measured simultaneously without the need of a field-free region near the target.

The dimensions of the detectors are chosen such that for central nucleus–nucleus collisions at 25 $A$GeV and a magnetic dipole field of $B = 1$ T about 70% of the emitted charged particles are accepted. Figure 8 displays a sketch of the proposed setup. The detector arrangement shown in figure 8 will be complemented by the HADES spectrometer which will be used to measure dileptons and hadrons at beam energies up to about 8 $A$GeV.

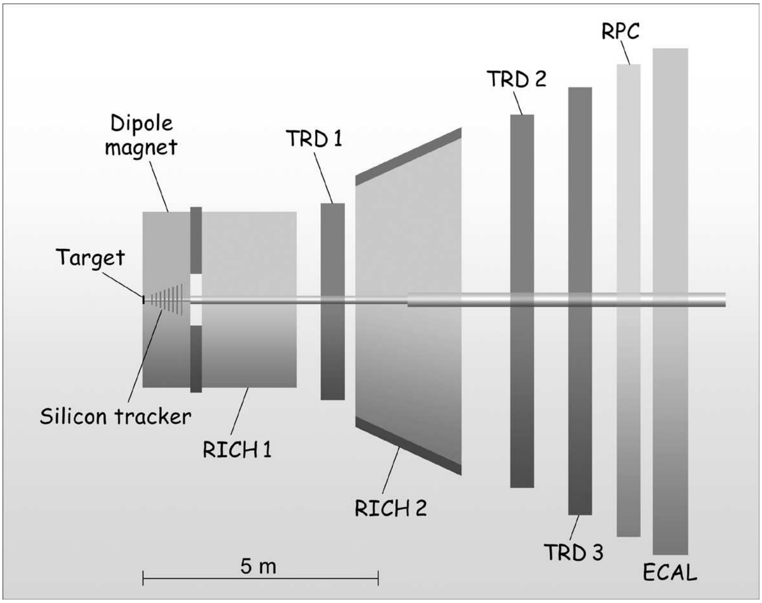


Fig. 8. Sketch of the planned Compressed Baryonic Matter (CBM) experiment. The beam enters from the left-hand side. The setup consists of a superconducting dipole magnet with a Silicon tracker System inside, a Rich Imaging Cherenkov detector (RICH) for electron identification, the first Transition Radiation Detector (TRD), the second RICH detector for high momentum particle discrimination (under investigation), the second and third TRD, the Time-Of Flight (TOF) wall which is a Resistive Plate Chamber (RPC) and the electromagnetic Calorimeter (ECAL) (from left to right). The total length of the setup is approximately 12 m from target at the entrance of the dipole to the ECAL.

The proposed experimental setup offers the possibility to determine particle multiplicities and phase-space distributions, the collision centrality and the reaction plane. The simultaneous measurement of electron–positron pairs and hadrons permits the study of cross correlations. This synergy effect opens a new perspective for the experimental investigation of nuclear matter under extreme conditions. Such systematic and detailed measurements include the variation of experimental conditions like beam energy and atomic number of the colliding nuclei and require a dedicated accelerator with high beam intensities, large duty cycle, excellent beam quality and high availability.

The following institutions participate in the CBM collaboration: IPNE Bucharest (Romania), Eötvös Univ. Budapest (Hungary), KFKI Budapest (Hungary), ISEC/LIP Coimbra (Portugal), Cyprus University Nikosia (Cyprus), GSI Darmstadt (Germany), JINR-LHE Dubna (Russia), JINR-LIT Dubna (Russia), JINR-LPP Dubna (Russia), Frankfurt University (Germany), INFN Catania (Italy), INFN Frascati (Italy), II. Phys. Inst. Univ. Heidelberg (Germany), KIP Univ. Heidelberg (Germany), Silesia Univ. Katowice (Poland), Shevshenko Univ. Kiev (Ukraine), Jagiellonian Univ. Krakow (Poland), Inst. of Computer Science V Mannheim Univ. (Germany), Inst. Phys. Marburg Univ. (Germany), INR Moscow (Russia), ITEP Moscow (Russia), SINP Moscow State Univ. (Russia), Kurchatov Inst. Moscow (Russia), Univ. Münster (Germany), Technical Univ. Prag (Czech Republic), IHEP Protvino (Russia), Univ. Pusan (Korea), Czech Academy of Sciences Rez (Czech Republic), IKHP Forschungszentrum Rossendorf (Germany), Univ. Santiago de la Compostela (Spain), Korea Univ. Seoul (Korea), KRI St. Petersburg (Russia), CKBM St. Petersburg (Russia) IN2P3-CNRS/ULP (IRes) Strasbourg (France), Nuclear Physics Division Warszawa Univ., (Poland), RBI Zagreb (Croatia).

## REFERENCES


[1] `http://www.gsi.de/GSI-Future/cdr/`

[2] F. Weber, *J. Phys. G: Nucl. Part. Phys.* **27**, 465 (2001).

[3] F. Wilczek, *Phys. Today*, **53**, 22 (2000).

[4] B. Friman, W. Nörenberg, V.D. Toneev, *Eur. Phys. J.* **A3**, 165 (1998).

[5] P. Senger, H. Ströbele, *J. Phys. G: Nucl. Part. Phys.* **25**, R59 (1999).

[6] Cern Courier Sept. 2003, p.17; V. Friese *et al.* [NA49 Collaboration], *J. Phys. G* **30**, S119 (2004).

[7] M. Gazdzicki, M. Gorenstein, *Acta Phys. Pol. B* **30**, 2707 (1999).

[8] E.L. Bratkovskaya *et al.*, `nucl-th/0307098`

[9] P. Braun-Munzinger *et al.*, *Phys. Lett.* **B465**, 15 (1999).

[10] J. Cleymans, K. Redlich, *Phys. Rev. Lett.* **81**, 5284 (1998).

[11] R. Stock, *Phys. Lett.* **B456**, 277 (1999).

[12] P. Braun-Munzinger, *Nucl. Phys.* **A681**, 119c (2001).

[13] Z. Fodor, S.D. Katz, *J. High Energy Phys.* **0203**, 014 (2002); *Phys. Lett.* **B534**, 87 (2002).

[14] D. Adamova *et al.* [CERES Collaboration], *Phys. Rev. Lett.* **91**, 042301 (2003).

[15] R. Rapp, J. Wambach, *Nucl. Phys.* **A661**, 33c (1999).

[16] F. Klingl *et al.*, *Phys. Rev. Lett.* **82**, 3396 (1999).

[17] C. Greiner, P. Koch, H. Stöcker, *Phys. Rev. Lett.* **58**, 1825 (1987).

[18] M. Iwasaki *et al.*, `nucl-ex/0310018`

[19] K. Rajagopal, *Nucl. Phys.* **A661**, 150c (1999).

[20] R. Vogt, *Phys. Rep.* **310**, 197 (1999).

[21] W. Cassing, E. Bratkovskaya, A. Sibirtsev, *Nucl. Phys.* **A691**, 74 (2001).